

Supplementary Information for

Solvate ionic liquids based on lithium bis(trifluoromethanesulfonyl)imide – glyme systems: coordination in MD simulation with scaled charges

Andreas Thum,^a Andreas Heuer,^a Karina Shimizu*^b and José Nuno Canongia Lopes^b

^aInstitut für Physikalische Chemie, Westfälische Wilhelms-Universität Münster,
Corrensstraße 28/30, 48149 Münster, Germany

^bCentro de Química Estrutural, Instituto Superior Técnico da Universidade de Lisboa,
Avenida Rovisco Pais 1, 1049 001 Lisboa, Portugal

Table S1: Densities of equimolar Li[NTf₂] + G3 and Li[NTf₂] + G4 mixtures from the previous [1] and present studies compared to other molecular dynamics simulations and experiments. All data in g cm⁻³.

Study	T / K	Li[NTf ₂] + G3	Li[NTf ₂] + G4
MD simulations			
Previous study [1]	303	1.472	1.436
Present study	298	1.474	1.437
Present study, non-reduced APCs	298	1.473	-
Tsuzuki <i>et. al</i> ^a [2]	303	1.43	1.41
Dong and Bedrov ^b [3]	303	-	1.41
Experiment			
Tamura <i>et. al</i> [4]	303	1.46	1.40
Yoshida <i>et. al</i> [5]	303	1.46	1.40
Zhang <i>et al</i> [6]	303	1.4247	1.4000

^aMD simulation; OPLS-AA and CL&P force field; charges as well as some Lennard-Jones and angle parameters reparametrized.
^bMD simulation; polarizable APPLE&P force field.

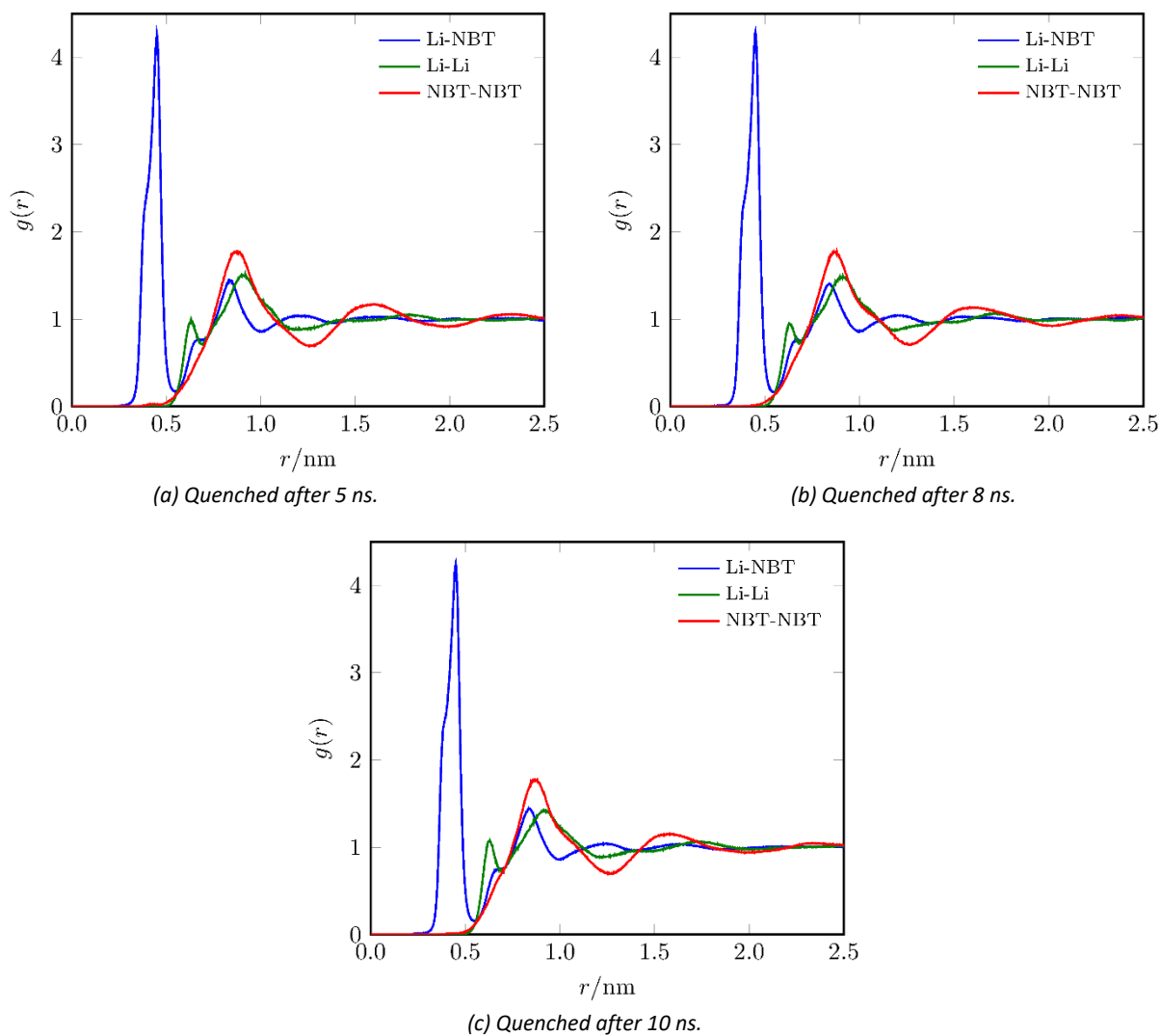


Figure S1: Radial distribution functions (RDFs), $g(r)$, of equimolar $\text{Li}[\text{NTf}_2] + \text{G3}$ mixtures obtained from three different simulations at 298 K. The starting structures were taken from snapshots of the production run at 500 K at 5 ns (a), 8 ns (b) and 10 ns (c). The RDFs of the simulation starting from the snapshot at 0 ns are shown in Figure 4b in the main text. Blue lines: RDFs between lithium cations (Li^+) and the nitrogen atom of bis(trifluoromethanesulfonyl)imide anions ($[\text{NTf}_2]^-$, NBT). Green lines: Li-Li RDFs. Red lines: NBT-NBT RDFs.

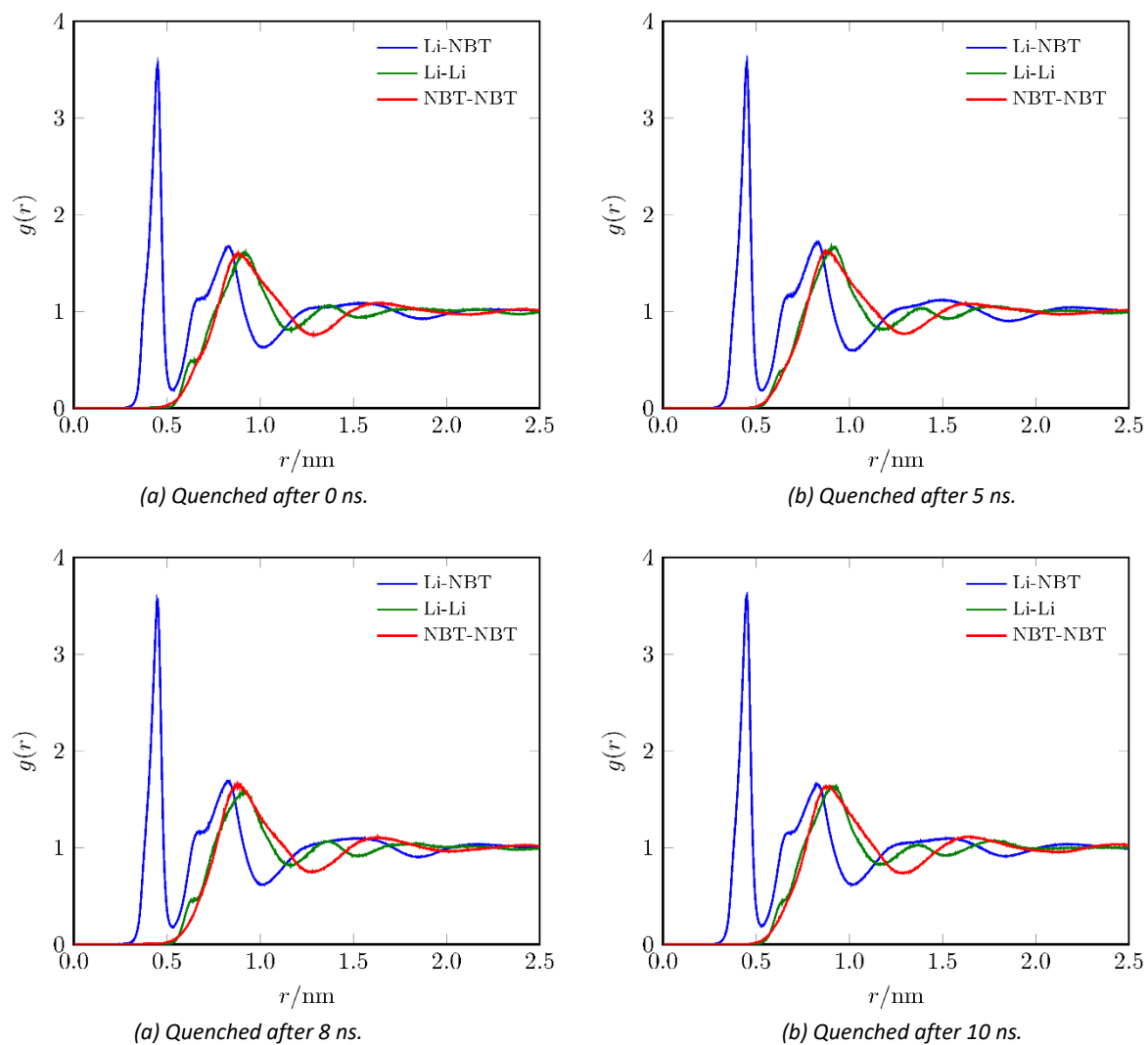


Figure S2: RDFs, $g(r)$, of equimolar $\text{Li}[\text{NTf}_2] + \text{G4}$ mixtures obtained from four different simulations at 298 K. The starting structures were taken from snapshots of the production run at 500 K at 0 ns (a), 5 ns (b), 8 ns (c) and 10 ns (d). Blue lines: RDFs between Li^+ and the nitrogen atom of $[\text{NTf}_2]^-$ (NBT). Green lines: Li-Li RDFs. Red lines: NBT-NBT RDFs.

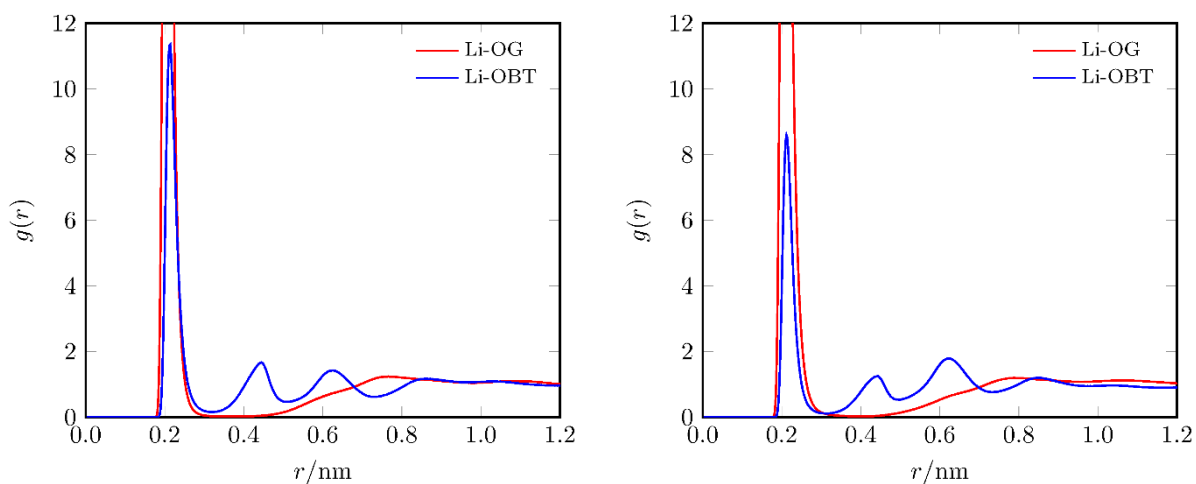


Figure S3: RDFs, $g(r)$, for equimolar mixtures of $\text{Li}[\text{NTf}_2] + \text{G3}$ (left) and $\text{Li}[\text{NTf}_2] + \text{G4}$ (right) at 298 K. Red lines: RDFs between Li^+ and the oxygen atoms of glyme (OG). Blue lines: RDFs between Li^+ and the oxygen atoms of $[\text{NTf}_2]^-$ (OBT).

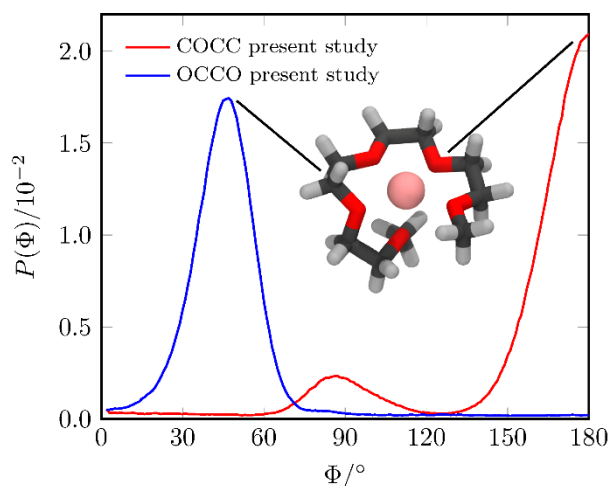


Figure S4: Dihedral probability distribution functions, $P(\phi)$, of selected COCC (red lines) and OCCO (blue lines) dihedral angles of G4 in equimolar mixtures of Li[NTf₂] + G4 at 298 K. The inset shows a representative simulation snapshot. Carbon atoms are displayed in black, oxygen atoms in red, hydrogen atoms in white and lithium atoms in pink. The maxima of the COCC and OCCO dihedral distributions are assigned to corresponding bonds in the molecule.

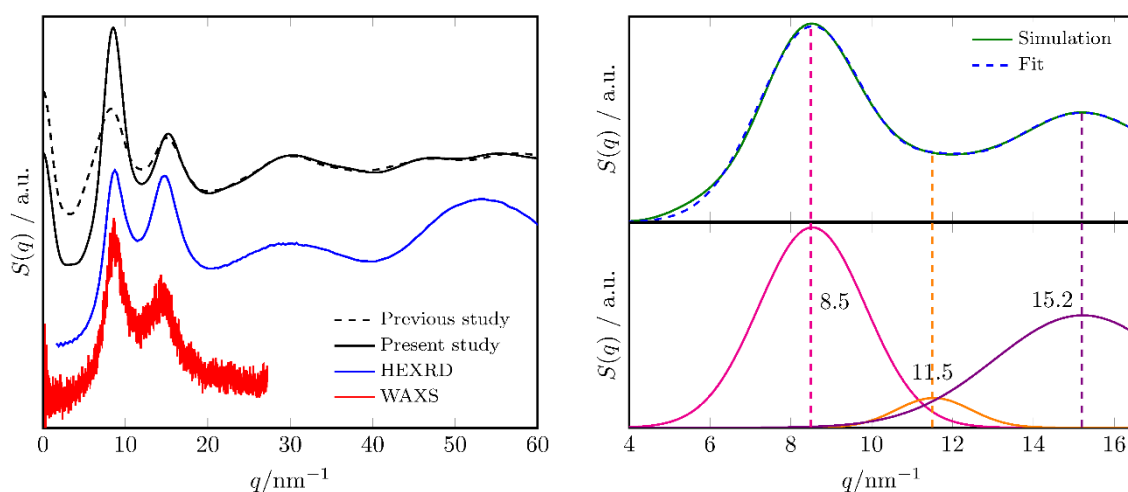


Figure S5: Total static structure factor functions, $S(q)$, of equimolar Li[NTf₂] + G3 mixtures. Left: Comparison of $S(q)$ between the previous [1] (dashed black line, at 303 K) and present study (solid black line, at 298 K) and with wide-angle X-ray scattering (WAXS, solid red line, at 298 K) and high-energy X-ray diffraction data [1] (HEXRD, solid blue line, at 298 K). Right: Multi-peak fitting of the new $S(q)$ in the $4 < q/\text{nm}^{-1} < 16.5$ region yielding three Gaussian functions. $S(q)$ was calculated in the same way as in the previous study.

Table S2: Peak positions of the total static structure factor functions, $S(q)$, of equimolar Li[NTf₂] + G3 mixtures derived from Gaussian deconvolution (see Figure S5, COP = charge-ordering peak). The experimental WAXS and HEXRD data are taken from the previous study [1]. All data in nm^{-1} .

	T / K	Contact peak	COP	Prepeak
Previous study [1]	303	15.0	11.8	8.2
Present study	298	15.2	11.5	8.5
WAXS [1]	298	14.2	11.1	8.6
HEXRD [1]	298	14.6	11.1	8.7

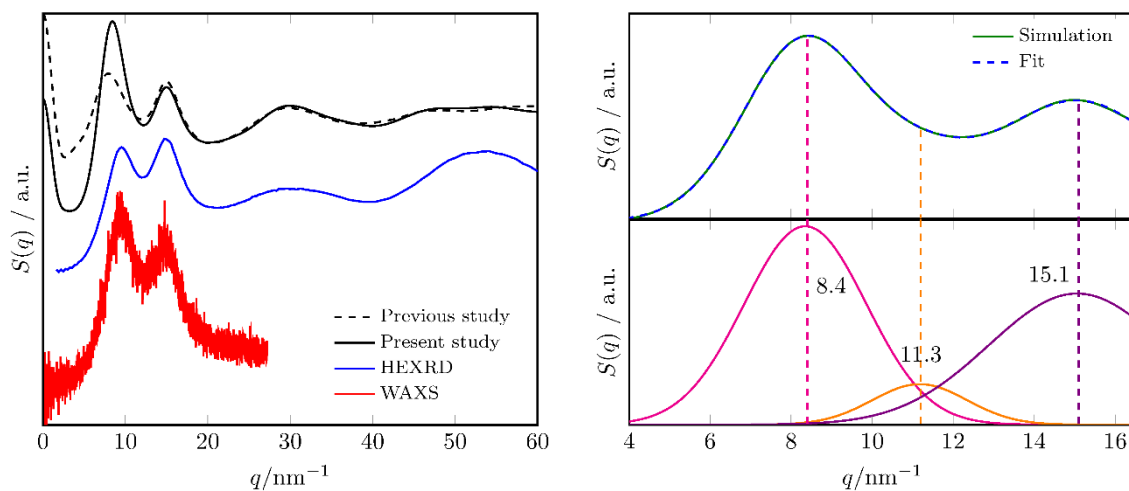


Figure S6: Total static structure factor function, $S(q)$, of equimolar $\text{Li}[\text{NTf}_2] + \text{G4}$ mixtures. Left: Comparison of $S(q)$ between the previous [1] (dashed black line, at 303 K) and present study (solid black line, at 298 K) and with WAXS (solid red line, at 298 K) and HEXRD data [1] (solid blue line, at 298 K). Right: Multi-peak fitting of $S(q)$ in the $4 < q/\text{nm}^{-1} < 16.5$ region yielding three Gaussian functions. $S(q)$ was calculated in the same way as in the previous study [1].

Table S3: Peak positions of the total static structure factor functions, $S(q)$, of equimolar $\text{Li}[\text{NTf}_2] + \text{G4}$ mixtures derived from Gaussian deconvolution (see Figure S6, COP = charge-ordering peak). The experimental WAXS and HEXRD data are taken from the previous study [1]. All data in nm^{-1} .

	T / K	Contact peak	COP	Prepeak
Previous study [1]	303	15.0	11.3	8.0
Present study	298	15.1	11.3	8.4
WAXS [1]	298	14.7	-	9.4
HEXRD [1]	298	14.9	11.0	9.1

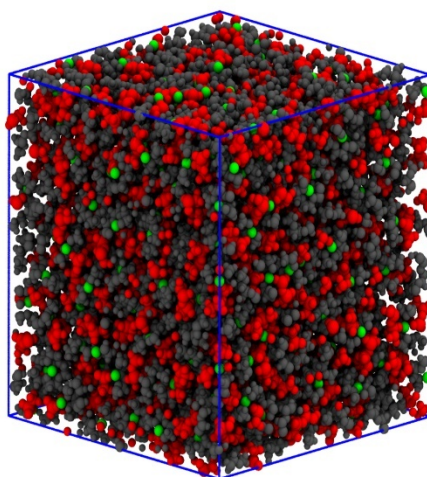


Figure S7: Snapshot of the simulation box of an equimolar $\text{Li}[\text{NTf}_2] + \text{G3}$ mixture at 298 K. Lithium cations are colored in green, all atoms belonging to $[\text{NTf}_2]^-$ anions are colored in red and all atoms belonging to G3 are colored in black.

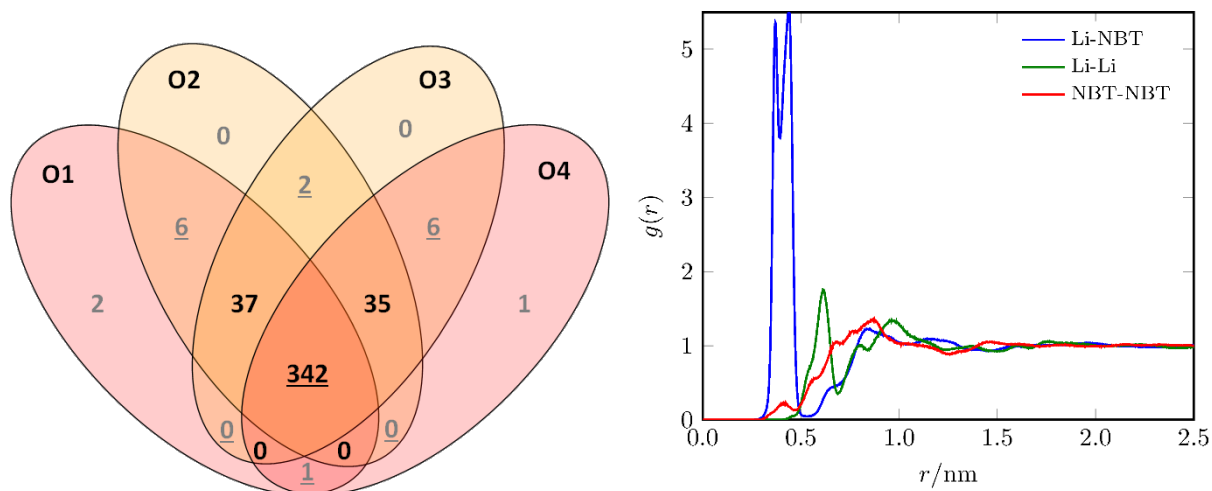


Figure S8: Venn diagram showing the connectivity between Li^+ and the four oxygen atoms of G3 (left) and RDFs, $g(r)$, (right) of an equimolar $\text{Li}[\text{NTf}_2] + \text{G3}$ mixture obtained from simulations with non-reduced APCs at 298 K. Blue line: RDF between Li^+ and the nitrogen atom of $[\text{NTf}_2]^-$ (NBT). Green line: Li-Li RDF. Red line: NBT-NBT RDF.

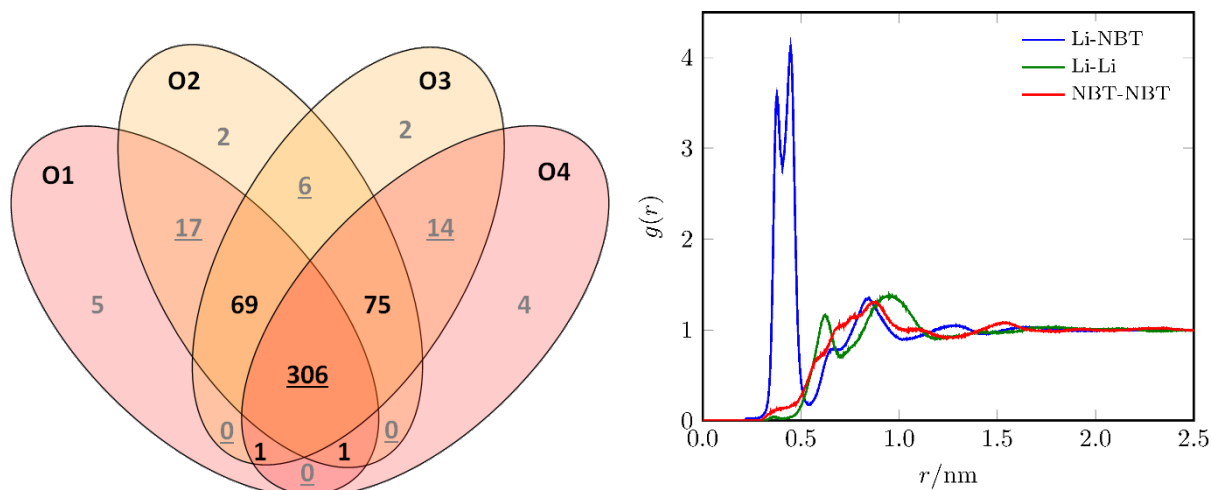
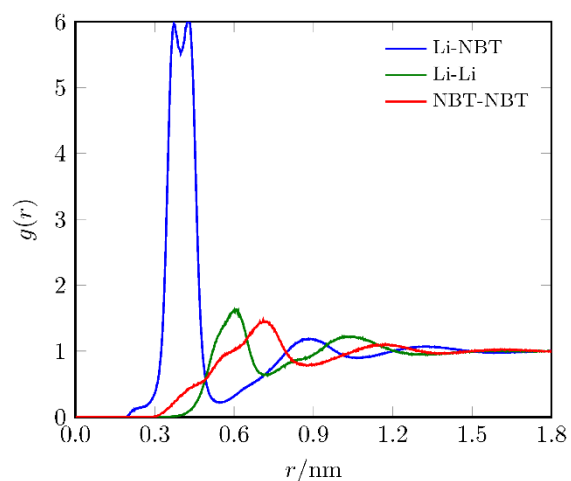


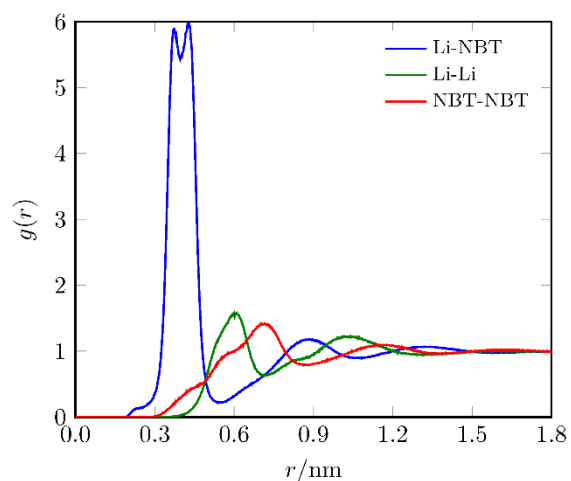
Figure S9: Venn diagram showing the connectivity between Li^+ and the four oxygen atoms of G3 (left) and RDFs, $g(r)$, (right) for an equimolar mixture of $\text{Li}[\text{NTf}_2] + \text{G3}$ obtained by extending the simulation of the previous study [1] by 8 ns at 303 K. Blue line: RDF between Li^+ and the nitrogen atom of $[\text{NTf}_2]^-$ (NBT). Green line: Li-Li RDF. Red line: NBT-NBT RDF.

Table S4: Average number of lithium-oxygen connections per lithium ion in an equimolar mixture of $\text{Li}[\text{NTf}_2] + \text{G3}$ obtained by extending the simulation of the previous study [1] by 8 ns at 303 K. $\text{Li-O}_{\text{anion}}$ and $\text{Li-O}_{\text{glyme}}$ denote the total number of Li-oxygen contacts established between Li^+ and $[\text{NTf}_2]^-$ or G3, respectively. Li-anion and Li-glyme stand for single Li-anion and Li-glyme contacts. $\text{Li-O}_{\text{total}}$ denotes the total number of Li-oxygen connections. Additionally, the amount of bidentate $[\text{NTf}_2]^-$ and the total numbers and percentages of $[\text{NTf}_2]^-$ and glyme molecules that are not attached to a lithium ion are given.

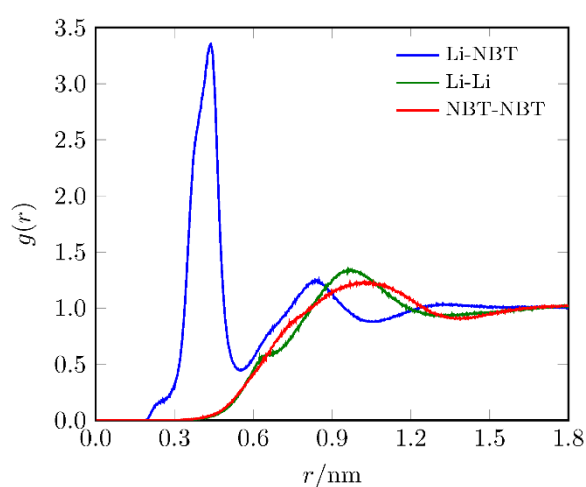
Previous study [1] extended by 8 ns	
Li-O_{anion}	2.13
Li-anion	1.77
Li-O_{glyme}	3.49
Li-glyme	0.99
Li-O_{total}	5.62
Bidentate $[\text{NTf}_2]^-$	20.3 %
Free $[\text{NTf}_2]^-$	35 (7.0 %)
Free glyme	18 (3.6 %)



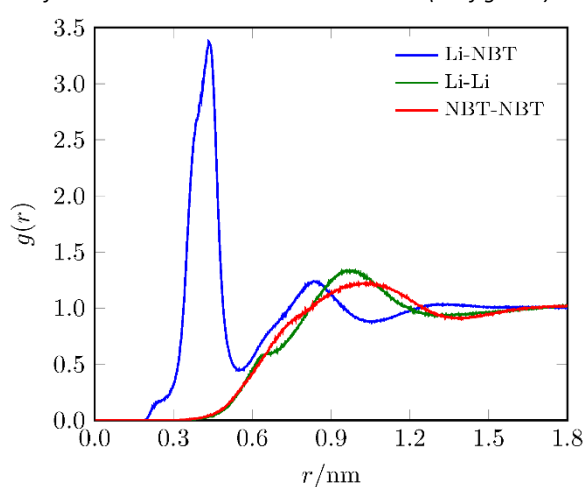
(a) Non-reduced APCs, random starting configuration.



(b) Non-reduced APCs, starting configuration taken from the simulation with reduced APCs (Subfigure c).



(c) Reduced APCs, random starting configuration.



(d) Reduced APCs, starting configuration taken from the simulation with non-reduced APCs (Subfigure a).

Figure S10: RDFs, $g(r)$, for equimolar mixtures of $\text{Li}[\text{NTf}_2] + \text{G3}$ obtained from simulations with non-reduced (a,b) and reduced (c,d) atomic point charges (APCs) at 700 K. Random starting configurations were used for (a) and (c). The starting configuration for (b) was taken from the simulation with reduced APCs and the one for (d) was taken from the simulation with non-reduced APCs. Blue lines: RDFs between Li^+ and the nitrogen atom of $[\text{NTf}_2]^-$ (NBT). Green lines: Li-Li RDFs. Red lines: NBT-NBT RDFs.

Table S5: Average number of lithium-oxygen connections per lithium ion in equimolar mixtures of Li[NTf₂] + G3 obtained from simulations with non-reduced (a,b) and reduced (c,d) APCs at 700 K. Random starting configurations were used for (a) and (c). The starting configuration for (b) was taken from the simulation with reduced APCs and the one for (d) was taken from the simulation with non-reduced APCs (see also description of Figure S10). Li-O_{anion} and Li-O_{glyme} denote the total number of Li-oxygen contacts established between Li⁺ and [NTf₂]⁻ or G3, respectively. Li-anion and Li-glyme stand for single Li-anion and Li-glyme contacts. Li-O_{total} denotes the total number of Li-oxygen connections. Additionally, the amount of bidentate [NTf₂]⁻ and the total numbers and percentages of [NTf₂]⁻ and glyme molecules that are not attached to a lithium ion are given.

	(a) Non-red. APCs	(b) Non-red. APCs	(c) Red. APCs	(d) Red. APCs
Start conditions	random	biased by (c)	random	biased by (a)
Li-O_{anion}	2.52	2.49	1.25	1.26
Li-anion	2.05	2.03	1.07	1.08
Li-O_{glyme}	2.42	2.45	3.28	3.27
Li-glyme	0.74	0.75	0.95	0.95
Li-O_{total}	4.94	4.94	4.53	4.53
Bidentate [NTf₂]⁻	22.9 %	22.7 %	16.8 %	16.7 %
Free [NTf₂]⁻	7 (1.4 %)	7 (1.4 %)	98 (19.6 %)	97 (19.4 %)
Free glyme	134 (26.8 %)	129 (25.8 %)	28 (5.6 %)	29 (5.8 %)

Table S6: Self-diffusion coefficients of Li⁺, [NTf₂]⁻ and G4 in equimolar mixtures of Li[NTf₂] + G4 in 10⁻⁷ cm² s⁻¹.

Study	T / K	D _{Li⁺}	D _{[NTf₂]⁻}	D _{G4}
MD simulations				
Reduced APCs	500	53	59	54
Shinoda et. al^a [7]	503	4.5	5.7	4.6
Tsuzuki et. al^a [2]	403	0.78	0.73	0.78
Dong and Bedrov^b [3]	303	0.41	0.4	0.41
Experiments				
Yoshida et. al^c [5]	500	67	58	71
Yoshida et. al^d [5]	303	1.31	1.22	1.29
Tamura et. al^d [4]	303	1.26	1.22	1.26
Zhang et. al^d [6]	303	1.26	1.22	1.26

^aMD simulation; OPLS-AA and CL&P force field; charges as well as some Lennard-Jones and angle parameters reparametrized.
^bMD simulation; polarizable APPLE&P force field.
^cExtrapolated via the Vogel-Fulcher-Tammann (VFT) equation.
^dPFM-NMR measurements

References

- (1) Shimizu, K.; Freitas, A. A.; Atkin, R.; Warr, G. G.; FitzGerald, P. A.; Doi, H.; Saito, S.; Ueno, K.; Umebayashi, Y.; Watanabe, M.; Canongia Lopes, J. N. *Phys. Chem. Chem. Phys.* 2015, 17, 22321–22335.
- (2) Tsuzuki, S.; Shinoda, W.; Matsugami, M.; Umebayashi, Y.; Ueno, K.; Mandai, T.; Seki, S.; Dokko, K. & Watanabe, M. *Phys. Chem. Chem. Phys.*, 2015, 17, 126-129
- (3) Dong, D.; Bedrov, D. *The Journal of Physical Chemistry B* 2018, 122, 9994–10004.
- (4) Tamura, T.; Yoshida, K.; Hachida, T.; Tsuchiya, M.; Nakamura, M.; Kazue, Y.; Tachikawa, N.; Dokko, K. & Watanabe, M. *Chemistry Letters*, 2010, 39, 753-755
- (5) Yoshida, K.; Tsuchiya, M.; Tachikawa, N.; Dokko, K.; Watanabe, M. *The Journal of Physical Chemistry C* 2011, 115, 18384–18394.
- (6) Zhang, C.; Ueno, K.; Yamazaki, A.; Yoshida, K.; Moon, H.; Mandai, T.; Umebayashi, Y.; Dokko, K. & Watanabe, M. *The Journal of Physical Chemistry B*, 2014, 118, 5144-5153
- (7) Shinoda, W.; Hatanaka, Y.; Hirakawa, M.; Okazaki, S.; Tsuzuki, S.; Ueno, K. & Watanabe, M. *The Journal of Chemical Physics*, 2018, 148, 193809